Characterization of Asphalt Concrete Microstructure using a Volumetrics-Based Thresholding Algorithm

Habtamu Zelelew[1] and Tom Papagiannakis[2]

ABSTRACT

This paper describes the implementation of a digital image processing (DIP) algorithm designed to automate the processing of asphalt concrete X-Ray computed tomography (CT) images. It involves circular cross section images of asphalt concrete (AC) cores of known volumetrics. Its innovation is that it uses the volumetric properties as the main criterion for establishing gray level thresholds for the boundaries between air-mastic and mastic-aggregates. The threshold values are established by minimizing the error between estimated core volumetric properties and the laboratory measured volumetric properties. The algorithm is referred to as volumetric-based global minima (VGM) thresholding. This method was implemented using MATLAB^{TM} routines for pre-processing and post-processing the X-Ray CT images. The data analyzed includes nine AC cores and their X-Ray CT images. Three mix designs and three aggregate types were used, all involving a PG 76-22 binder. Each core was imaged through 148 sections perpendicular to its axis (i.e., 1 mm distance increments). Post-processing of the rectangular section images enhanced separation between adjacent aggregates. The final images produced are significantly improved compared to the raw X-Ray CT images. The algorithm was shown to produce realistic renderings of the microstructure of asphalt concretes. Their quality is sufficient for input into numerical simulations of AC micromechanical behavior. This algorithm was shown to be a major improvement over the largely manual techniques used in the past.

Keywords: Asphalt concrete, digital image processing, and microstructure.

[1] (Corresponding Author) Visiting Assistant Professor, University of Minnesota Duluth, Department of Civil Engineering, 1303 Ordean Court, Duluth, MN 55812, Phone: (218)-726-8427, Fax: (218)-726-8581, E-mail: hzelelew@d.umn.edu

[2] R.F. McDermott Professor and Chair, Department of Civil and Environmental Engineering University of Texas at San Antonio, One UTSA Circle, San Antonio, TX 78249, Phone: (210)-458-7517, Fax: (210)-458-6475 , E-mail: at.papagiannakis@utsa.edu

INTRODUCTION

Asphalt concrete (AC) mixtures are heterogeneous materials consisting of air voids, aggregates and mastics. Mastics consist of binder and fines passing sieve size 75 micron. The overall performance of ACs depends to a large extent on their internal microstructure, that is the way these three phases are distributed and interact with each-other. Imaging techniques have been used effectively for studying the microstructure of ACs. Effectively capturing the AC microstructure is also essential for modeling their mechanical behavior using numerical techniques. A number of recent studies have utilized X-Ray computed tomography (CT) for capturing and characterizing the AC microstructure (Yue et al., 1995; Masad et al., 1999; Shashidhar, 1999; Masad et al., 2001; Masad et al., 2002; Tashman et al., 2002; Wang et al., 2004).

The majority of the studies highlighted above use a combination of digital image processing (DIP) and manual/subjective techniques for processing AC images in a format suited to numerical simulation. DIP techniques include image contrast enhancement, image noise removal, thresholding, edge detection and image segmentation. Typically, the gray level threshold that separates aggregates from mastics referred to as thresholding is selected subjectively. Additional pixel modifications are required to adjust the relative proportions of aggregate and mastic to reflect the actual volumetrics of the AC (Papagiannakis et al., 2002). Isolating the air phase further complicates the problem. To date, there have been few attempts to fully automate this process (Yue et al., 2003; Offrell and Magnusson, 2004).

An automated method was developed for the processing of AC X-Ray CT images (Zelelew and Papagiannakis, 2008). Its key feature is that it performs gray level thresholding on the basis of the volumetric properties of the mix. It establishes gray threshold values between air-mastic and mastic-aggregate by minimizing the error between the relative volume of the gray image and the corresponding property of the AC core. The method, referred to as a volumetrics-based global minima (VGM) thresholding algorithm, is fully described in Zelelew (2008). It applies to images of sections of AC cores taken perpendicular to the axis at regular distance intervals. Its advantage is that it can efficiently provide representations of the AC microstructure, while preserving the volumetric properties of the mix. As a result, it is suited for capturing the AC microstructure for numerical simulation purposes.

OBJECTIVE

This paper has two objectives:

- Demonstrate the application of the VGM thresholding algorithm in effectively processing a large number of X-Ray CT images.
- Use these images to study AC microstructure properties such as mixture proportions and distributions.

EXPERIMENTAL DATA

The data analyzed consisted of an AC mixture and its X-Ray CT images is part of a Texas DOT funded study (Alvarado et al., 2007). The samples were prepared by the University of Texas-El Paso and X-Ray CT scanning took place at Texas A&M University. A summary of the background information for this data is given below.

A total of nine AC cores was produced, each involving a combination of three different mix designs and three different aggregate types. The mix designs included are Coarse Matrix High Binder Type C (CMHB-C), Porous Friction Course (PFC), and Superpave Type C (Superpave-C). Three aggregate types were used, namely hard limestone (HL), granite (G), and soft limestone (SL). The binder grade used for all these samples was a PG 76-22. The gyratory compacted specimen, 150 mm diameter by 165 mm height was cored and sawn to a diameter of 100 mm and a height of 150 mm, resepectively.

The type of facility required and the procedure used for capturing AC images using X-Ray CT is well documented (Masad et al., 2002). Each of the nine AC cores was scanned perpendicular to its axis at 1 mm distance interval to yield 148 slices per core, ignoring the top and bottom slices. Figure 1 shows the raw format of one of these images consisting of 512 x 512 pixels. The resulting resolution is 195 micron per pixel. A summary of the background information for this data can be found in Zelelew (2008).

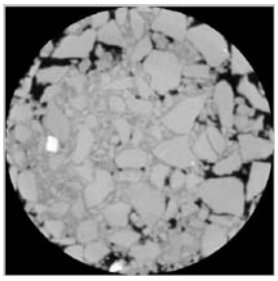

Figure 1. Example of Raw Image; HL CMHB-C Core.

OVERVIEW OF THE VGM ALGORITHM

An automated digital image processing (DIP) technique called volumetric-based global minima (VGM) thresholding algorithm was proposed to process AC X-ray CT images (Zelelew and Papagiannakis, 2008). VGM was utilized to process the horizontally sliced X-Ray CT images. The method is based on identifying gray level boundary thresholds between air, mastic and aggregate phases with reference to volumetric information. VGM has three inter-related stages. The first stage involves image pre-processing for contrast enhancement and noise removal. The second stage is the main thresholding routine accepting as input the enhanced images of the first stage and volumetric information for the AC. It consists of two components, namely volumetrics-driven thresholding and three-dimensional representation/sectioning. The third stage further enhances particle separation through edge detection and image segmentation techniques. Implementation of VGM to study AC microstructure is described below.

IMPLEMENTATION OF THE VGM ALGORITHM

Image Pre-Processing

Typically, raw X-Ray CT images have poor contrast and include a variety of types of noise. Its main sources are sensor quality, as well as image digitizing and pre-processing. Variations in densities within the individual mastic and aggregate also contribute to image noise. Improving image contrast and reducing noise is essential in obtaining enhanced image quality. X-ray CT images of AC core sections consist of pixel representations that vary in gray level between 0 and 255 (i.e., black and white, respectively). An example of such a raw image is shown in Figure 2a.

Image contrast can be improved using an image contrast enhancement technique called histogram equalization. This method distributes the gray level intensity of pixels uniformly throughout the image. The MATLAB^{TM} built-in function *histeq* was used for this purpose (Misiti et al., 2009). To reduce AC X-Ray CT image noise, the median filtering technique was utilized. Figure 2b shows the enhanced image using the histogram equalization method. Figure 2c shows an example of image noise reduction using median filtering using a kernel of 3x3 pixels. Comparing Figures 2a, 2b, and 2c suggests that the pre-processing stage significantly enhances image quality.

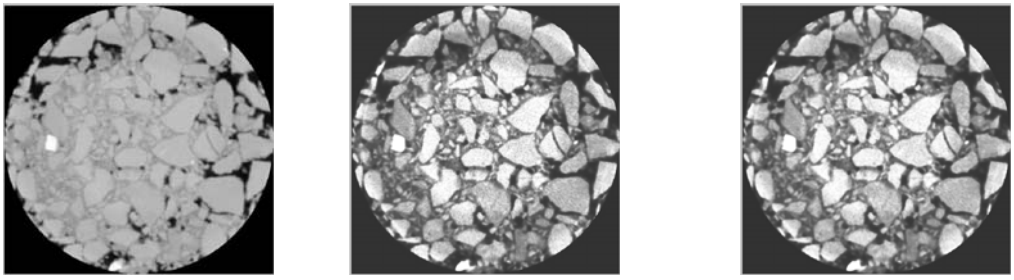

(a) **(b)** **(c)**

Figure 2. Example of Pre-Processing an Image of the HL CMHB-C Core; (a) Raw Image; (b) Contrast Enhanced Image; (c) De-noised Image.

Thresholding

The main VGM thresholding algorithm developed seeks to establish two gray level thresholds, a lower threshold T_1 corresponding to the air void-mastic boundary, and a higher threshold T_2 corresponding to the mastic-aggregate boundary. Finding these thresholds, within the 0 to 255 range, involves an iterative process, whereby a gray level threshold value is assumed, and the corresponding area proportions for each core section are computed and combined into an estimated average volumetric property for the core. The threshold values selected are those that minimize the error between estimated and actual volumetric properties.

Applying the thresholding methodology yielded the two thresholding boundaries for each of the AC cores tested, namely T_1 and T_2. In performing these calculations, it was assumed that the mastic contains all the fines that cannot be detected by the image resolution (i.e., for this dataset sizes finer than 195 micron).

The actual boundary gray levels are illustrated in Figures 3 and 4 for T_1 and T_2, respectively. The highest T_1 value was observed for the Superpave-C mix with the hard

limestone aggregate, while the lowest was for the CMHB-C with soft limestone and PFC with hard limestone aggregate. The highest T_2 value was observed for the CMHB-C mix with the hard limestone aggregate, while the lowest was for the PFC mix with the granite aggregate. Table 1 summarizes the errors between the laboratory measured and VGM estimated volumetric properties. The maximum errors observed were 1.43%, 4.33% and 0.92%, respectively. These results suggest that the VGM algorithm is quite accurate in preserving mix volumetric properties.

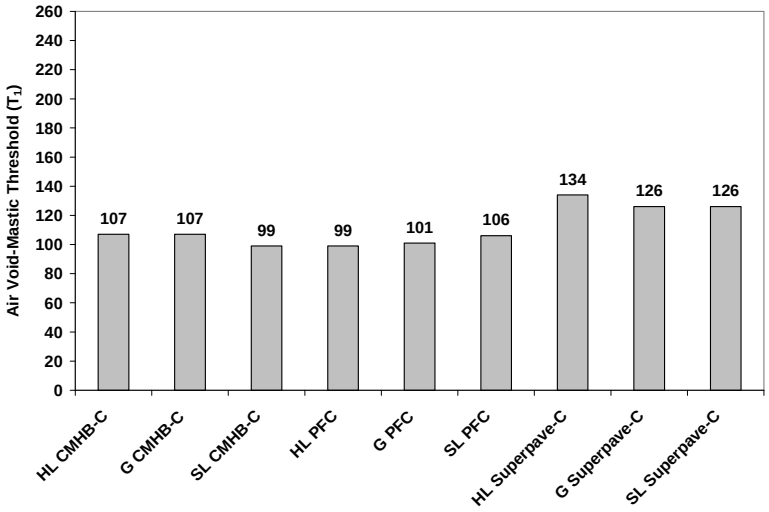

Figure 3. Air Void-Mastic Boundary Threshold (T_1).

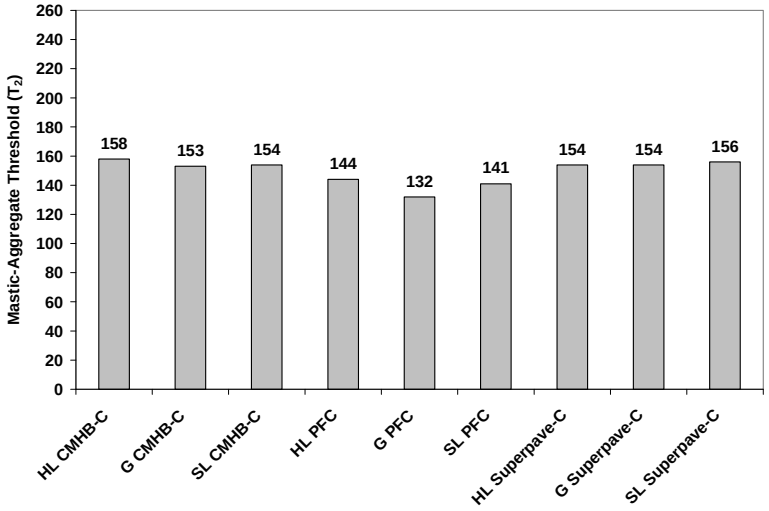

Figure 4. Mastic-Aggregate Boundary Threshold (T_2).

Table 1. Comparison of Laboratory Measured and VGM Estimated Mixture Proportions.

Mixture ID	Air Void (%)		Absolute Error (%)	Mastic (%)		Absolute Error (%)	Aggregate (%)		Absolute Error (%)
	Measured	Estimated		Measured	Estimated		Measured	Estimated	
HL CMHB-C	7.30	7.32	0.26	16.98	17.07	0.49	75.72	75.61	0.14
G CMHB-C	6.90	6.89	0.19	17.72	18.19	2.66	75.38	74.92	0.61
SL CMHB-C	7.00	6.99	0.17	18.33	18.85	2.86	74.67	74.16	0.69
HL PFC	19.50	19.42	0.39	14.78	14.98	1.33	65.72	65.60	0.18
G PFC	19.60	19.71	0.58	14.34	14.58	1.63	66.06	65.71	0.53
SL PFC	19.30	19.37	0.38	15.42	15.29	0.81	65.28	65.34	0.08
HL Superpave-C	7.40	7.42	0.31	16.81	17.14	1.98	75.79	75.44	0.47
G Superpave-C	6.90	6.96	0.87	17.39	16.64	4.33	75.71	76.41	0.92
SL Superpave-C	6.70	6.60	1.43	17.84	18.40	3.15	75.46	75.00	0.62

HL: Hard Limestone; G: Granite; and SL: Soft Limestone

Image Post-Processing

Studying Figure 5d points to the need for image post-processing to separate aggregates contacting each-other (e.g., refer circled aggregates). This problem needs to be resolved prior to using these images in numerical simulations. Image post-processing was carried out through edge detection and segmentation. The rectangular sections obtained needed enhancement to improve separation between adjacent particles. It was carried out through edge detection techniques using Canny edge operator (Canny, 1986). It is based on the first derivative of gray intensity, but it retains only derivatives that exceed a threshold value. Image segmentation consists of partitioning mixture components into distinct regions (i.e., in this case air voids, mastics and aggregates). Segmentation was carried out using watershed transformations to separate overlapping (or touching) mastic and aggregate objects. It was performed using morphological dilation and erosion operations through MATLAB™ (Misiti et al., 2009). Figure 6 shows an example of this operation for the HL CMHB-C core. Figures 6a, 6b, and 6c show the mastic phase, the aggregate phase, and the entire mixture, respectively. Comparing Figure 5d, Figure 6b shows the improved separation between aggregate, as a result of post-processing. Similar processing was carried out for all nine core images. The VGM software and the associated pre-processing and post-processing routines can be made available on request.

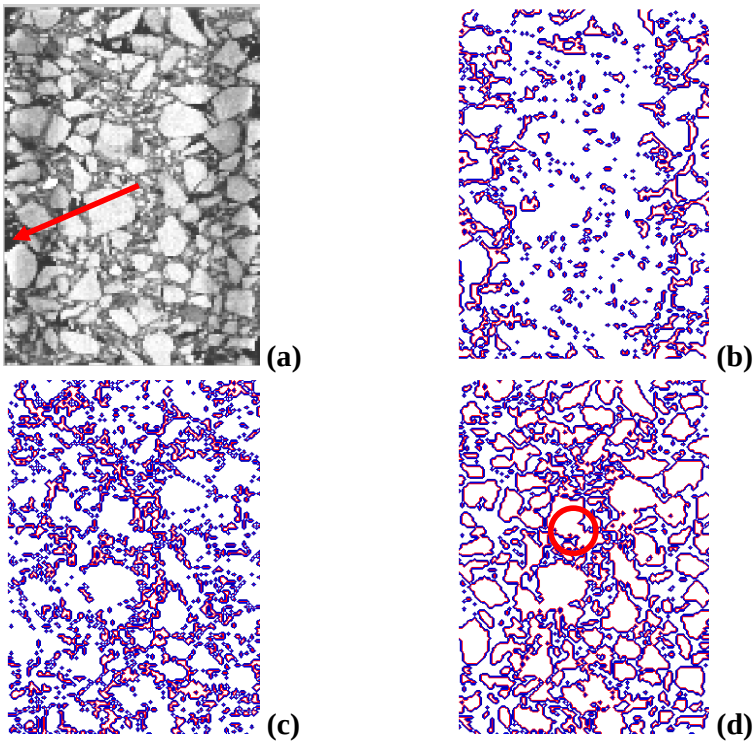

Figure 5. Representation of the HL CMHB-C Core Sections Prior to Image Post-Processing; (a) Image after Thresholding, (b) Air Phase, (c) Mastic Phase, and (d) Aggregate Phase.

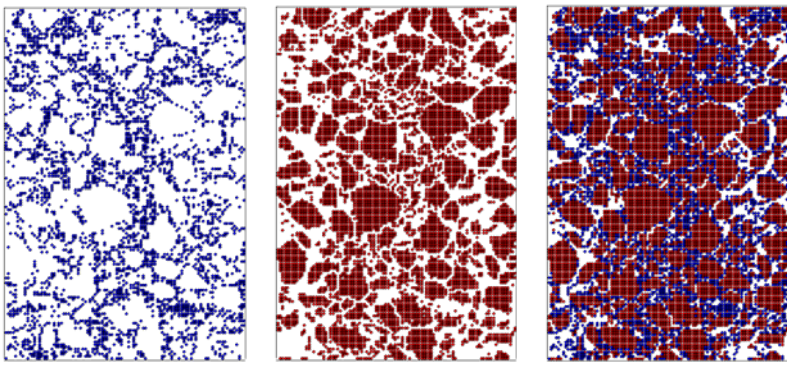

(a) **(b)** **(c)**

Figure 6. Representation AC Rectangular Sections for Numerical Modeling/Simulation, (a) Mastic Phase in Blue, (b) Aggregate Phase in Red, and (c) Mixture; HL CMHB-C.

SUMMARY AND CONCLUSION

This paper presented the results of implementing the VGM algorithm on a large dataset of AC X-Ray CT images. It provided examples from each step of the algorithm, namely, image contrast enhancement, noise reduction, thresholding, edge detection and segmentation. Analysis of the 2-D rectangular sections assembled from the circular sections revealed that the air-mastic gray threshold is relatively insensitive to the air void content, while the mastic to aggregate gray threshold increases with decreasing aggregate volume. The three Superpave mixtures exhibited the lowest mastic volume proportions, while the porous friction course mixtures exhibited the highest aggregate volume proportions. Post-processing of the rectangular section images improved separation between adjacent aggregates. The final images produced are significantly improved compared to the raw X-Ray CT images. The algorithm was shown to produce realistic renderings of the microstructure of asphalt concretes. Their quality is sufficient for input into numerical simulations of AC micromechanical behavior. This algorithm was shown to be a major improvement over the largely manual techniques used in the past. Therefore, researchers and State highway agencies can implement the approach for pavement modeling and quality control/assurance (QC/QA) purposes.

ACKNOWLEDGMENT

Sincere thanks are expressed to Dr. Masad of Texas A&M University and to Dr. Nazarian of University of Texas-El Paso for supplying the asphalt concrete X-Ray CT images and the AC volumetric information, respectively.

REFERENCES

1. Alvarado C., Mahmoud, E., Abdallah, I., Masad, E., Nazarian, S., Langford, R., Tandon, V., and Button, J. (2007) "Feasibility of Quantifying the Role of Coarse Aggregate Strength on Resistance to Load in HMA. TxDOT Project No. 0-5268 and Research Report No. 0-5268.
2. Canny, J. (1986) "A Computational Approach to Edge Detection". IEEE Transactions on Pattern Analysis and Machine Intelligence, 8 (6), 679-698.
3. Masad, E., Jandhyala, V.K., Dasgupta, N., Somadevan, N., and Sashidhar, N. (2002) "Characterization of Air Voids Distribution in Asphalt Mixes using X-Ray Computed Tomography". Journal of Materials in Civil Engineering, 14(2), pp. 122-129.
4. Masad, E., Muhunthan, B., Shashidhar, N., and Harman, T. (1999) "Internal Structure Characterization of Asphalt Concrete using Image Analysis". Journal of Computing in Civil Engineering, 13(2), pp. 88-95.
5. Masad, E., Somadevan, N., Bahia, H.U., and Kose, S. (2001) "Modeling and Experimental Measurements of Strain Distribution in Asphalt Mixes". Journal of Transportation Engineering, 127(6), pp. 477-485.
6. Misiti, M., Misiti, Y., Oppenheim, G., and Poggi, J.M. (2009) "MATLAB Program". The Math Works, Inc., Natick, Massachusetts.
7. Offrell, P., and Magnusson, R. (2004) "In Situ Photographic Survey of Crack Propagation in Flexible Pavements". International Journal of Pavement Engineering, 5 (2), pp. 91-102.
8. Papagiannakis A.T., A. Abbas, and Masad, E. (2002) "Micromechanical Analysis of the Viscoelastic Properties of Asphalt Concretes". Transportation Research Record 1789, Transportation Research Board, National research Council, Washington DC, pp. 113-120.
9. Shashidhar, N. (1999) "X-Ray Tomography of Asphalt Concrete". Transportation Research Record 1681, Transportation Research Board, National Research Council, Washington, D.C., 186-192.
10. Tashman, L., Masad, E., Angelo, J. D., Bukowski, J., and Harman, T. (2002) "X-ray Tomography to Characterize Air Void Distribution in Superpave Gyratory Compacted Specimens". International Journal of Pavement Engineering, 3(1), pp. 19-28.
11. Wang, L.B., Paul, H.S., Harman, T., and Angelo, J.D. (2004) "Characterization of Aggregates and Asphalt Concrete Using X-Ray Computerized Tomography: A State-of-The-Art Report". Journal of the Association of Asphalt Paving Technologists, 73, pp. 467-500.
12. Yue, Z.Q., Bekking, W., and Morin, I. (1995) "Application of Digital Image Processing to Quantitative Study of Asphalt Concrete Microstructure". Transportation Research Record 1492, Transportation Research Board, National Research Council, Washington, D.C., pp. 53-60.
13. Yue, Z.Q., Chen, S., and Tham, L.G. (2003) "Finite Element Modeling of Geomaterials using Digital Image Processing". Computers and Geotechnics, 30, pp. 375-397.
14. Zelelew, H.M., and Papagiannakis, A.T. (2008) "A Volumetrics-based Thresholding Algorithm for Processing Asphalt Concrete X-Ray CT Images". International Journal of Pavement Engineering (accepted in-press).
15. Zelelew, H.M. (2008) "Simulation of the Permanent Deformation of Asphalt Concrete Mixtures Using Discrete Element Method (DEM)". PhD Dissertation, Washington State University, Pullman, USA.